Design and Implementation of Scalable Wireless Sensor Network for Structural Monitoring

Shamim N. Pakzad[1]; Gregory L. Fenves[2]; Sukun Kim[3]; and David E. Culler[4]

Abstract: An integrated hardware and software system for a scalable wireless sensor network (WSN) is designed and developed for structural health monitoring. An accelerometer sensor node is designed, developed, and calibrated to meet the requirements for structural vibration monitoring and modal identification. The nodes have four channels of accelerometers in two directions and a microcontroller for processing and wireless communication in a multihop network. Software components have been implemented within the TinyOS operating system to provide a flexible software platform and scalable performance for structural health monitoring applications. These components include a protocol for reliable command dissemination through the network and data collection, and improvements to software components for data pipelining, jitter control, and high-frequency sampling. The prototype WSN was deployed on a long-span bridge with 64 nodes. The data acquired from the testbed were used to examine the scalability of the network and the data quality. Robust and scalable performance was demonstrated even with a large number of hops required for communication. The results showed that the WSN provides spatially dense and accurate ambient vibration data for identifying vibration modes of a bridge.

Introduction

Structural health monitoring (SHM) is a rapidly developing field encompassing the technology and algorithms for sensing the state of a structural system, diagnosing the structure's current condition, performing a prognosis of expected future performance, and providing information for decisions about maintenance, safety, and emergency actions (Farrar 2001; Doebling et al. 1996; Lynch and Loh 2006). Advances in micro-electro-mechanical-systems (MEMS) technology in the past decade provide opportunities for sensing, wireless communication, and distributed data processing for a variety of new SHM applications. There have been several prototypes of sensor networks, emphasizing the sensing devices, such as Wang and Pran (2000), Westermo and Thompson (1997), and Zimmermann (1999); wireless communication, such as Ihler et al. (2000), Paek et al. (2005) and Pei et al. (2005); and data processing for SHM, such as Williams and Messina (1999), Strubbs et al. (1999), and Sohn and Farrar (2000). The rapid reduction in physical size and cost of MEMS-based wireless sensors has driven increased interest in the scalability of wireless sensor networks (WSN) to hundreds or even thousands of nodes.

While the current research in SHM has made substantial progress, the scalability of the WSN for structural monitoring applications has not been thoroughly investigated or demonstrated. Wireless communication is essential for scalability because installation and maintenance of a monitoring system with a wired or tethered communication network would be too expensive and complex for hundreds to thousands of nodes. Scalability of a wireless sensor network involves the sensors, data acquisition and processing, and wireless communication. A scalable network is one that can be expanded in terms of the number of sensors, complexity of the network topology, data quality (e.g., sampling rate, sensor sensitivity), and amount of data while the cost of the expansion (installation and operational cost, communication time, processing time, power, and reliability) is no worse than a linear, or nearly linear, function of the number of sensors. WSN scalability needs to consider an integrated view of the hardware and software. For hardware, scalability involves sensitivity and range of MEMS sensors, communication bandwidth of the radio, and power usage. The software issues include reliability of command dissemination and data transfer, management of large volume of data, and scalable algorithms for analyzing the data. The combined hardware-software issues include high-frequency sampling, which is necessary for structural health monitoring, and the tradeoffs between on-board computations compared with wireless communication between nodes. Addressing these problems is essential for the application of WSN beyond laboratory prototypes to the scale needed for structural monitoring applications.

Wireless sensor networks have been developed for a variety of purposes that range from low duty-cycle, low-power environmental monitoring applications, such as described by Mainwaring et al. (2002) and Tolle et al. (2005), to high-fidelity applications (accurate measurements, high sampling rate, lossless communication) for monitoring of mechanical and structural systems. Mastroleon et al. (2004) examined the architecture of a wireless

[1]Doctoral Student, Dept. of Civil and Environmental Engineering, Univ. of California, Berkeley, CA 94720 (corresponding author). E-mail: shamimp@ce.berkeley.edu

[2]Professor, Dept. of Civil and Environmental Engineering, Univ. of California, Berkeley, CA 94720.

[3]Doctoral Student, Dept. of Electrical Engineering and Computer Sciences, Univ. of California, Berkeley, CA 94720.

[4]Professor, Dept. of Electrical Engineering and Computer Sciences, Univ. of California, Berkeley, CA 94720.

system for SHM with an emphasis on low-power multisensor modular units. Ruiz-Sandoval et al. (2006) developed a MEMS-based accelerometer and strain sensor board for a WSN for structural health monitoring using Mica motes for communication and control. Maser et al. (1996) described the field deployment of a wireless sensor network on a highway bridge. The wireless transceiver used one-hop communication with a base station, and the base stations were interconnected using cellular telephony. Lynch et al. (2003) examined the quality of data from a seven-node wireless network with MEMS accelerometers by comparison with conventional wired accelerometers. Lynch et al. (2005) presented the deployment of 14 wireless sensors to monitor forced acceleration response of Geumdang Bridge in Korea. These studies have been advances in wireless sensor networks for structural health monitoring, but since the systems rely on one-hop wireless communication between a sensor and a base station, the studies do not address the question of scalability.

The objective of this paper is to present the design, development, and large-scale deployment and testing of a scalable wireless sensor network for structural health monitoring. The key technology innovations are: (1) a new approach for maximizing the effective network bandwidth with a large number of communication hops; and (2) reliable command dissemination and data transfer for high-frequency sampling, all using a low-power microcontroller and radio. Both aspects use multihop communication between nodes, which is essential for scalable networking because the radio power required for single-hop communication in a large network is impractical. The first section of the paper presents the requirements and design for the WSN architecture, describes the hardware and software components, and summarizes the calibration of the system. The second section describes the network topology and deployment of the scalable WSN for a long-span bridge, analyzes the network performance, and presents ambient vibration data of the bridge. The third section describes the algorithms used to analyze the data and presents information about the spatial sampling of the vibration properties of the bridge. The paper concludes with recommendations for achieving scalability in wireless sensor networks.

Wireless Sensor Network Architecture

The first step in designing a sensor network is deciding on the physical quantities to measure. In the case of a structure as a dynamic system, the measurement of acceleration is the most straightforward, but is recognized that acceleration is an indirect function of damage and structural condition. Although sensing displacement is possible [using global positioning system (GPS) technology, for example], the reliability, accuracy, and sampling rate are not yet sufficient for many applications, particularly those needing high-frequency sampling of small displacements. Strain measurements could provide a direct measure of damage, but the installation, operation, and interpretation of reliable strain sensors on a large structure is difficult. Consequently, accelerations provide useful information about structural vibration characteristics, so they are adequate for the primary goal of this investigation, which is to examine the scalability of wireless sensor networks. For bridge applications, the accelerometer range should be large enough to capture $1-2$ g during an earthquake, yet they should be sensitive enough to measure ambient vibrations due to wind and traffic on the order of tens to hundreds of μg.

The network must be designed for fast sampling rates for temporal scalability, and reliable command dissemination and data
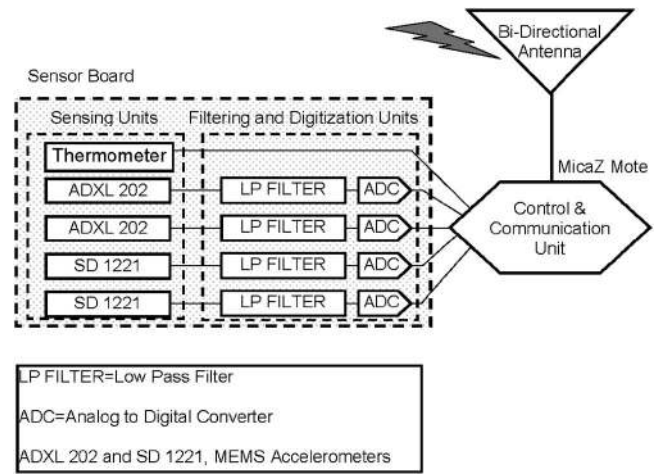

Fig. 1. Schematic diagram of sensor node

collection over many nodes to provide spatial scalability. Considering the sampling rate for accelerations or other structural response quantities, the lower vibration frequencies of a structure are generally on the order of $10^{-1}-10^{+1}$ Hz, but higher sampling rates are desirable for two reasons. Local features of response are characteristic of much higher vibration frequencies and, second, high-frequency sampling can be used to reduce noise and increase the signal-to-noise ratio (Oppenheim and Schafer 1999). High-frequency sampling, however, complicates time synchronization of nodes over the network and may generate large volumes of data that need to be managed, processed, and possibly transmitted.

Another design requirement is that the network must have high communication reliability to transmit data and disseminate commands without loss of information (packet loss). Particularly for rare events, such as an earthquake, data loss is not acceptable. For ambient vibration applications, data loss would have the affect of increasing the noise, which would make modal identification more difficult. In this work the requirement of no data loss is adopted.

High-frequency sampling, multihop communication, and reliable data transmission are stringent requirements. The following subsections provide details about how the hardware and software components of the scalable WSN are designed to address these requirements.

Sensor Node Hardware Design

The network consists of a set of sensor nodes, and each node has three main hardware components, sensors, filters and microcontroller, and radio for wireless communication. Fig. 1 is a schematic of the major components of a node. For the measurement of low-level and high-level accelerations, two commercially available MEMS accelerometer sensors are used each in two directions (one horizontal and one vertical). The use of two sensor types is a cost-effective solution and allows examination of performance-price tradeoffs. The high-level sensor is Analog Device's ADXL202, a widely used device that provides a ±2 g range with a sensitivity of 1 mg at 25 Hz (Analog Devices 1999). For low-level ambient vibrations, a Silicon Design 1221L provides acceptable sensitivity for ambient structural vibrations at a relatively low cost (Silicon Designs 2007). Tests show that the Silicon Design accelerometers have a hardware noise ceiling of 10 μg
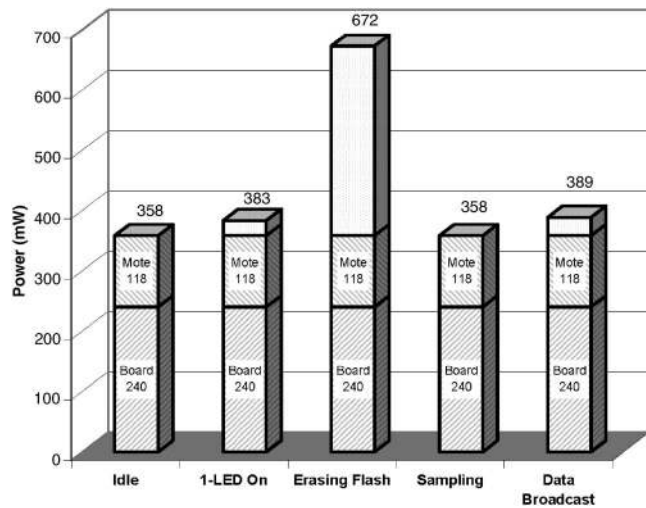
Fig. 2. Power consumption of sensor node in operational modes

Fig. 3. Software architecture of TinyOS components for reliable and high-frequency sampling wireless network

(Pakzad and Fenves 2004). (Pakzad et al. 2005), which is small enough to resolve signals with amplitude of a few hundreds of μg.

Each channel from the MEMS accelerometers provides an analog voltage that is fed to a single-pole anti-aliasing low-pass filter with a cutoff frequency of 25 Hz. The filter was set for a long-span bridge application because even very high vibration modes have frequencies well below the anti-aliasing filter. The filtered analog signal is fed to a 16-bit analog-to-digital converter (ADC) for each of the four channels. Sampling is done at a high frequency (1 kHz), but the digitized signal is downsampled by averaging, which acts as a digital filter and reduces the Gaussian noise level by a factor of $\sqrt{n}$, when every n sample is averaged. This analog anti-aliasing filter at 25 Hz, high-frequency sampling at 1,000 Hz, and downsampling to 50 Hz provide a simple and power-efficient approach for high-resolution acceleration measurements.

For each node, a mote with a microcontroller provides local processing and storage capability and a low-power radio communication. The MicaZ mote was selected because it has a good tradeoff between processing and communication capability, and power requirements (Crossbow 2007a). The MicaZ has 512 kB flash memory, which can store up to 250,000 2-byte data samples, and a 2.4 GHz radio-frequency (RF) Chipcon CC2420 transceiver with a hardware interface that can support commercially available bi-directional antennas. The ability of the mote to connect with a bi-directional antenna was an important factor because the long-span bridge application required a linear topology and a standard omni-directional antenna would have wasted a significant amount of radio power.

Power consumption is a critical factor in scalability of wireless sensor networks. To analyze power for the sensor node with the MicaZ mote, Fig. 2 shows the power draw for the major components of the node in various operational modes based on a 9 V power source. The power consumption of the sensor board (MEMS sensors, anti-aliasing filters, and ADC) is more than twice that of the MicaZ mote. This is a result of a design decision made to use a single power regulator for the node. An improved, but more complex, hardware design would have separate power regulators for the sensors and mote, thus allowing the mote to operate while the sensors are in a sleep mode. Fig. 2 shows that the mote draws a significant portion of power while idle because
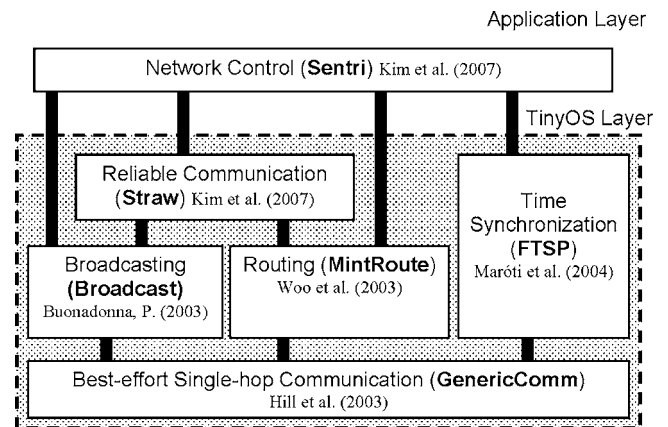
the radio is in a listening mode. The broadcast mode only increases the power consumption by about 10%. The test data were consistent with the specification sheet that estimates that the radio uses 62 mW in the listening mode versus 57 mW in broadcast mode (Chipcon Products 2007). Based on the power usage testing of the node, it was decided to use four 6 V lantern batteries to provide 12 V and 15 A-h in the deployment.

An alternative to the MicaZ mote would have been iMote2, which has similar functionality as MicaZ but consumes more power. Crossbow (2007a,b) estimates power consumption of 24 mW for MicaZ in active mode with an 8-bit bus size and 8 MHz clock speed versus 139.5 mW for iMote2 with 32-bit bus size and 12 MHz clock speed. The greater computational power of iMote2, however, does not make a critical difference in the performance of the node for the bridge testbed application. The power consumption was the principal factor in the selection of the mote.

System Software

The system software for a scalable wireless sensor network is based on the TinyOS operating system (TinyOS 2007) an open-source, framework for programming Mica motes (Hill et al. 2000). TinyOS is multilevel component-oriented software that supports a wide variety of applications for wireless sensor networks. Low-level components perform basic tasks, and higher-level components use sequences of low-level components to achieve more complex functionality while maintaining efficiency and simplicity of coding. The components range from providing simple diagnostic operations such as turning an indicator light emitting diode (LED) on/off, to sophisticated components for routing of data packets in a self-configuring wireless communication network. With this background, Fig. 3 shows the system software architecture and the main components of the TinyOS operating system and application layer that were developed or adapted for scalable structural health monitoring. The important components are discussed in the following subsections.

Multihop Communication

A focus of the recent work on WSN has been on multihop communication. Multihop communication is the transfer of data and commands between two nodes that are not in the direct radio range, using intermediary nodes. Multihop communication is essential for scalability of low-power wireless sensor networks be-

T: One-packet one-hop transfer time   n: number of the hops
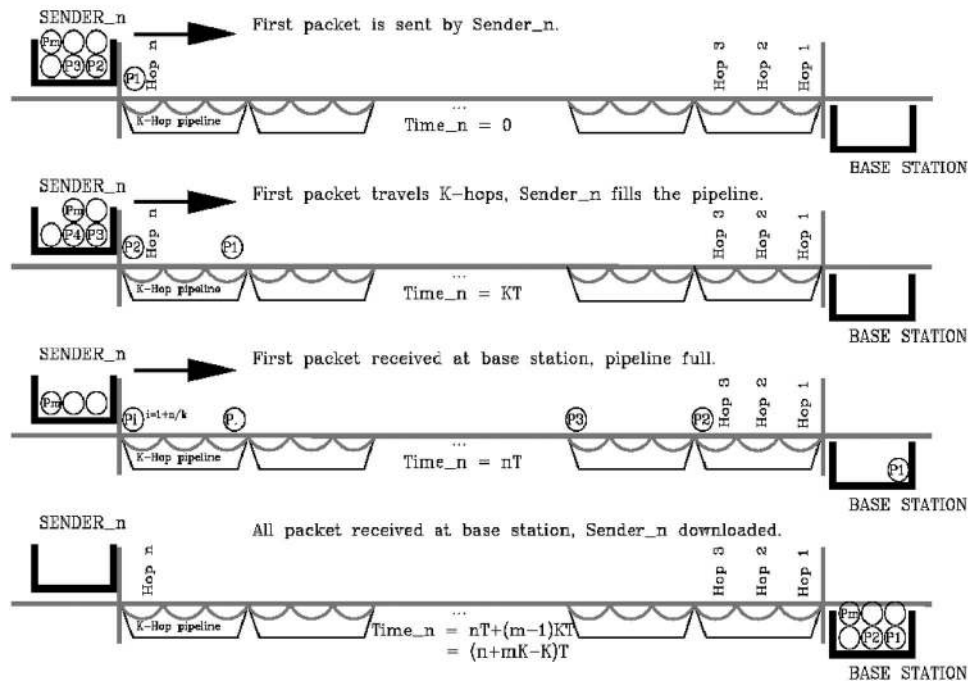
m: number of the packets   K: pipeline length

Fig. 4. Transfer time for n-hop network using pipelining

cause single-hop networks are spatially limited by the radio range and cannot span long distances without a large power supply. However, multihop presents major challenges to several aspects of a WSN. The routing of data packets in a single-hop network only needs a queue for all of the nodes to transmit their packets directly to a base station. In a multihop network, routing is more complex because each node has to determine how to find the most efficient way to forward packets to the base station and coordinate transmission of packets received from other nodes. The routing needs to reconfigure dynamically for robustness if a node fails and is no longer able to serve as an intermediary (such as because of radio interference) for multihop communication.

One of the most important aspects of a multihop network is establishing and updating the routing information (typically referred to as routing tables or charts) for each node to communicate with the base station. The TinyOS component MintRoute (Woo et al. 2003) provides multihop connectivity in the wireless network. MintRoute establishes the routing of packets by minimizing the power cost of the multihop travel of a packet from a generating node to the base station, subject to a constraint on minimally acceptable transmission quality for each one-hop link. If a link falls below a threshold quality level, MintRoute seeks an alternative route that bypasses the weak link with the minimum power requirement. The TinyOS component GenericComm provides low-level communication between a node and one nearby node that requires the least amount of power (Hill et al. 2003). The component Broadcast (Buonadonna 2003) builds upon GenericComm to provide radio connectivity between the two nodes.

Data Pipelining

Each node in a multihop network has two functions. Its first function is to generate data by sampling and sending data packets to the base station through the network. A node also acts as an intermediary relay by receiving data packets generated by other nodes and passing them towards the base station. Spatial reuse of network bandwidth is essential for a scalable multihop network. Bandwidth reuse by pipelining means that several nodes in addition to the one that generated the data, transmit packets at the same time within a network. Although this increases the amount of data communicated within the network, pipelining must be designed so that the nodes transmitting simultaneously do not interfere with each other. Single-hop networks cannot reuse bandwidth because only one node broadcasts at any time to the base station. Pipelining significantly increases the effective bandwidth of large networks by maintaining a higher throughput for the network regardless of the number of hops.

Fig. 4 illustrates how pipelining allows packets from a node to travel through different parts of the network at the same time, thus increasing the effective bandwidth of the network. The parameter K=number of hops between transmitting nodes. If $K=n$, where n=number of hops in the route, there is no pipelining and the sender waits until the first packet is received by the base station before sending another packet. As K decreases, pipelining reuses more of the bandwidth, but with an increased potential for radio interference. The interference causes a higher rate of packet loss and data retransmission, thus reducing bandwidth. In the limit, K has a lower bound of 3 because radio interference would jam the network if $K=2$, and $K=1$ is not possible.

For a multihop network without pipelining ($K=n$) the total transfer time for m packets from a sender that is n hops away from the base station is mnT, where T=transfer time of one packet for one hop. Pipelining with a length K reduces this time to $(n+mK-K)T$. The effective bandwidth of a network with a pipeline length of $K<n$ to a network without pipelining ($K=n$) is

$$\frac{\text{bandwith with pipelining}}{\text{bandwith without pipelining}} = \frac{\dfrac{1}{(n + mK - K)T}}{\dfrac{1}{mnT}}$$

$$= \frac{mn}{mK + n - K} \xrightarrow[m \text{ large}]{} \frac{n}{K}$$

The increase in bandwidth is significant for a network with large number of hops, n, and using a small pipeline length K.

To provide spatial reuse of bandwidth in a multihop wireless sensor network, Kim et al. (2006) developed a new TinyOS component for data pipelining. The length K is selected based on the link quality and radio interference. In this application, K is set when the routing table is established and held constant. Additional work by Kim et al. (2006) extends pipelining to set the optimal value of K in different parts of a network dynamically.

Reliable Data Communication

Even with multihop routing and data pipelining in a wireless sensor network, data packets will be lost because of electromagnetic interference and collision of packets that arrive at a node at the same time. In many applications it is not critically important if a small percentage of packets are lost, but for SHM it is vital to have a protocol that guarantees reliable transmission of data because features of the response characteristics may be affected by data loss. Furthermore, for monitoring critical events such as an earthquake, data loss is also unacceptable because of the value of the information. The challenge is to provide reliability with minimal network resources, in terms of computation and memory, and hence power. To satisfy the requirement of reliable data communication, a new protocol, scalable thin and rapid amassment without loss (Straw) was developed, tested, and deployed. It is a selective negative-acknowledgement (NACK) collection protocol, in which the data transfer is always initiated by the receiver. The sender transmits the data when it is requested by the receiver, and the receiver then identifies and returns a list of missing packets back to the sender. The sender retransmits those packets again until all packets are received. Straw provides reliable data transfer when the sender and receiver are separated by an arbitrary number of communication hops (Kim et al. 2007).

Time Synchronization and Jitter Control

Multihop networks have to perform time synchronization. In a single-hop network this is a trivial task since the base station sends a start command and all of the nodes receive it virtually at the same time. The roundtrip communication time from a node to the base station over multiple hops needs to be accurately estimated for efficient transmission, recognizing that the time is nondeterministic in a multihop network. This problem is addressed by a global synchronized clock mechanism with time stamping and regression algorithms (Maróti et al. 2004).

Jitter is the distortion of a signal caused by variance in the time-sampling interval as a result of poor synchronization. Ying et al. (2005) explains how accurate jitter control is essential for high-frequency sampling, since asynchronous data can produce errors in identifying the mode shapes of a structural system. As illustrated in the schematic shown in Fig. 5, there are two sources of jitter: temporal and spatial. Temporal jitter occurs at a node when the sampling intervals are not uniform due to uneven clock ticks, event handling, or other hardware bias. Spatial jitter is the time-synchronization error between different nodes, which occurs

because of uncertainty in estimating latency in propagating a global time across the network and the drift of the clock at a node.

To provide time synchronization in a network by controlling jitter, a TinyOS component named flooding time-synchronization protocol (FTSP) is used. FTSP propagates the global time generated by the base station through the network by a series of handshakes between adjacent nodes, until the entire network is in the same time zone. Experiments by Maróti et al. (2004) show that the protocol limits the spatial jitter to 67 μs over a network of 59 nodes and 11 hops. High-frequency sampling and logging can increase this jitter, so Kim et al. (2007) performed a jitter analysis and the tests showed that the temporal jitter using the Timer component of TinyOS is limited to 10 μs for a sampling rate of up to 6.67 kHz. For a harmonic signal of 25 Hz, the highest frequency of interest in the current application, this time synchronization error causes a maximum 0.16% error in the measured value of the signal. For an ambient acceleration signal of 10 mg amplitude, the jitter is equivalent to 16 μg noise level, which falls below the sensitivity of the MEMS accelerometers.

The jitter analysis of the nodes with FTSP provided insight into the limitations of the motes for a WSN in structural health monitoring. While the MicaZ microcontrollers are faster than the flash memory, other microcontroller tasks are delayed because of sampling, which is a time-consuming operation and thus blocking computation and communication. Using multiplexed ADC with its own clock would marginally limit temporal jitter, but at the cost of consuming additional power for the separate clock. A faster microcontroller would have smaller jitter but still have the same fundamental problem that would need to be addressed.

Network Control

For structural health monitoring, Kim et al. (2007) developed an application named Sentri, based on TinyOS, for high-level control of a wireless network from a base station. The control program consists of two components: one for the individual nodes and the second one for the base station. The node software allows the mote to listen to the network, join the network, control the sensor board (sampling, filtering, logging), and be a sender/receiver for multihop communication. It is designed for a very small memory footprint because of the limited resources for the motes. The base station control software has more functionality for sending inquiries to all nodes in the network, evaluating connectivity and communications, and executing commands on parts or the entire network.

Testing and Calibration

The sensor nodes, network, and the system software were tested by several laboratory and field experiments to determine sensitivity of the sensors, communication reliability and bandwidth, and the robustness of the system components. Pakzad et al. (2005) describe these tests, which included quiet-environment tests to determine the noise floor of the MEMS accelerometers, shaking table tests to asses the accuracy of the sensors over a wide frequency range, and a variety of field tests to study the multihop networking and reliable data collection components. Each sensor node was individually calibrated by a rotary tilt table and shift and scale factors for converting the ADC output to acceleration were determined for all channels.

Full-Scale Deployment on Long-Span Bridge

Long-span, suspension bridges have been the subject of study for structural health monitoring because they are important physical
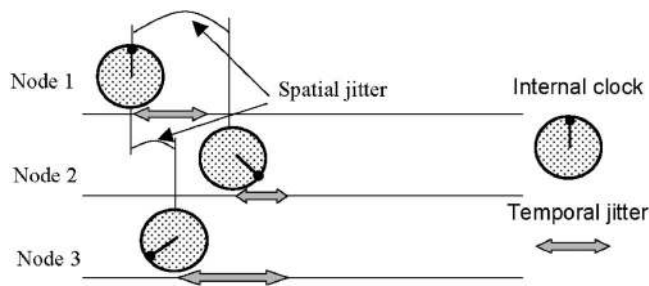
Fig. 5. Spatial and temporal sources of jitter

infrastructure and can have unique vibration properties and response to earthquake ground motion. As two examples of studies using data from wired sensors, Smyth et al. (2003) examined the Vincent Thomas Bridge in the 1987 Whittier and 1994 Northridge earthquakes with linear and nonlinear system identification techniques to develop a multiinput, multioutput dynamic model of the bridge using data from 26 accelerometer sensors on the superstructure and the footings. Abdel-Ghaffar and Scanlan (1985a,b) used spectral densities and ambient vibration data caused by wind and traffic and collected at 28 locations on the span and a tower of the Golden Gate Bridge to estimate vibration frequencies and mode shapes of the bridge.

Building upon the Abdel-Ghaffar and Scanlan study, the Golden Gate Bridge was selected for the full-scale deployment of the scalable wireless sensor network described in the previous sections. The bridge has a main-span (1,280 m), two side-spans (342.9 m), and two towers (210.3 m above the water level). The objective of the WSN deployment was to identify the vibration characteristics of the main span and the south tower. The deployment on the Golden Gate Bridge provided the opportunity to test

the WSN in a difficult environment and with a linear topology that required a large number of hops for communication.

Fig. 6 shows the instrumentation plan for the bridge with a total of 64 nodes, 56 on the main span (measuring transverse and vertical acceleration) and eight on the South Tower (measuring transverse and longitudinal acceleration). On the main span 53 nodes were deployed on the west side, and three nodes on the east side. Each main span node was attached to the top flange of the floor girder directly inside of the cable. Fig. 7 shows a node with the bidirectional antenna, along with the clamps and guy wires for temporary installation of the testbed. The node spacing on the west side was selected based on the range of the radio with a majority of nodes placed 30.5 m apart, but at places where an obstacle obstructs a clear line of sight this distance was reduced to 15.25 m. The three nodes on the east side, added in the second phase after changing the batteries, were located at the two quarter spans and the midspan of the bridge. The east side nodes have radio communication with the west side nodes under the roadway deck. For the South Tower, there is a node on each side of each strut. The tower nodes have a clear line of sight between them and hence have greater radio range than the main-span nodes. The node on the west side of the strut above the superstructure collects data from all the nodes on the tower and transmits them to the network on the main-span.

Installation of the network began on July 14, 2006 and the last set of data was collected on September 22, 2006. The 512 kB flash memory of each node can buffer about 250,000 samples of data, which can be allocated to any combination of the five sensor channels on the node (four accelerometers and a temperature sensor). Each run starts with a pause to synchronize the network and disseminate a command to start sampling at a future time. After the scheduled sampling takes place there is a pause to establish the network routing. The recorded data are then transferred from
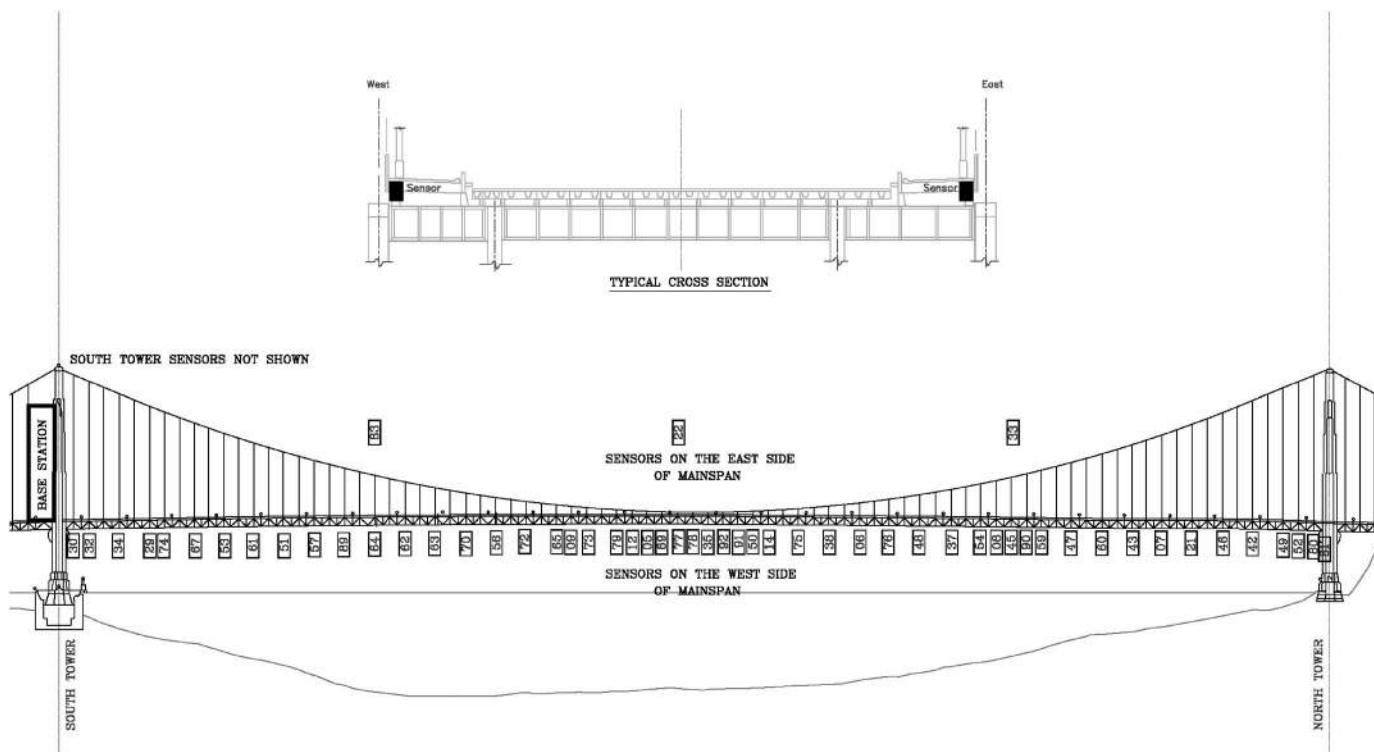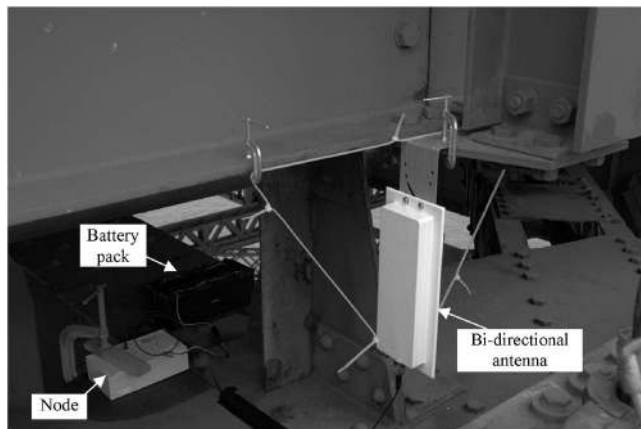

Fig. 6. Instrumentation plan for 56 nodes on main span of the Golden Gate Bridge

Fig. 7. Node with its battery pack and bi-directional antenna on main span of the Golden Gate Bridge

each node to the base station using the reliable data communication and pipelining. A complete cycle of sampling and data collection for the full network produces 20 MB of data and takes about 9 hours. There were a total of 174 such runs during the deployment. This total includes runs where the network was being installed and tested so all of the collected data sets do not contain data from all of the nodes.

The network was fully installed on the west side of the main span and the south tower on August 1, 2006 and 13 sets of data were collected with the first set of batteries. At the time of changing batteries on September 22, 2006, the nodes on the east side of the main span were installed and three more sets of data collected. The runs include a variety of combinations of sensor channels, which always included the two low-level Silicon Design 1221 accelerometers, but the other two high-level ADXL202 accelerometers and the temperature sensor were turned off in some of the runs to reduce the volume of the data or increase the sampling rate.

Ambient Vibration Data

As an example of the ambient vibration data, the vertical accelerations from the low-level accelerometers in a typical run (174) are shown in Figs. 8–10 for the three quarter points on the main-span. The sampling frequency was 50 Hz over 1,600 s, resulting in 80,000 samples per channel. Each figure includes plots of the signal and the power spectral density (PSD) using the Welch method (Welch 1967).

The amplitudes of the ambient accelerations are about ±10 mg, but spikes of up to 50 mg are apparent, presumably caused by heavy vehicles traveling on the roadway. The PSD plots show clear and consistent peaks at frequencies at several nodes. These spectral peaks are distinct in lower frequencies. Twenty peaks are visible in the frequency plots, which correspond to vertical and torsional vibration mode shapes of the bridge, as will be shown later. The PSD plots indicate that the low-frequency noise level is very small compared with the peaks of the spectra (the power of the noise is about two orders of magnitude smaller than the power at peak frequencies).

Wireless Network Performance

Three aspects of the wireless communication performance for the network were examined empirically using data from the bridge:
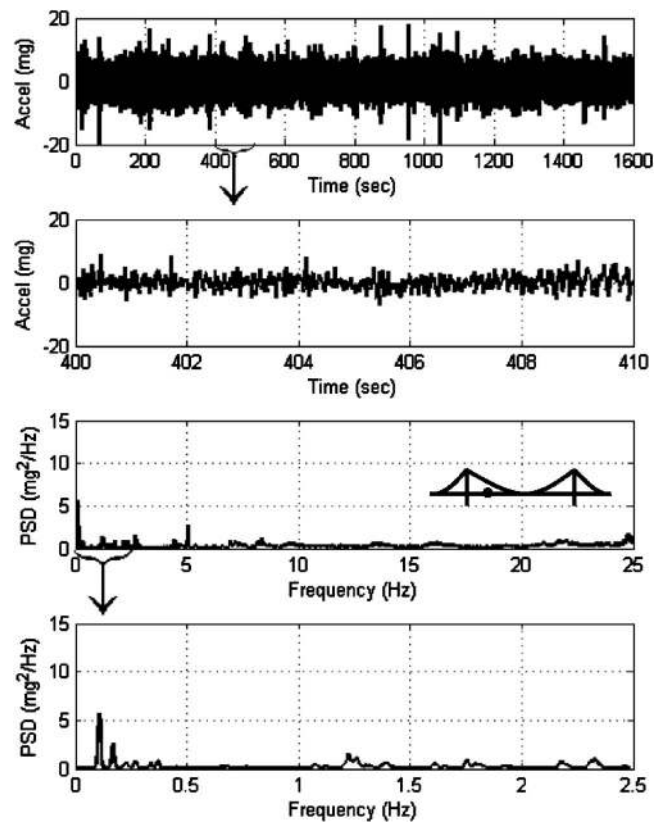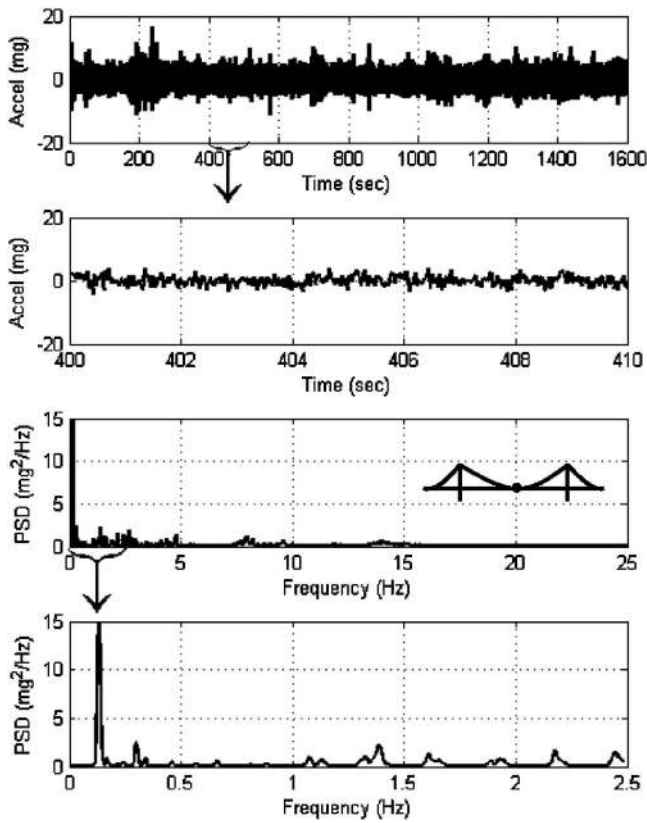

Fig. 8. Time-history and power spectral density for vertical sensor at west-side south 1/4-span (run 174, node 64)
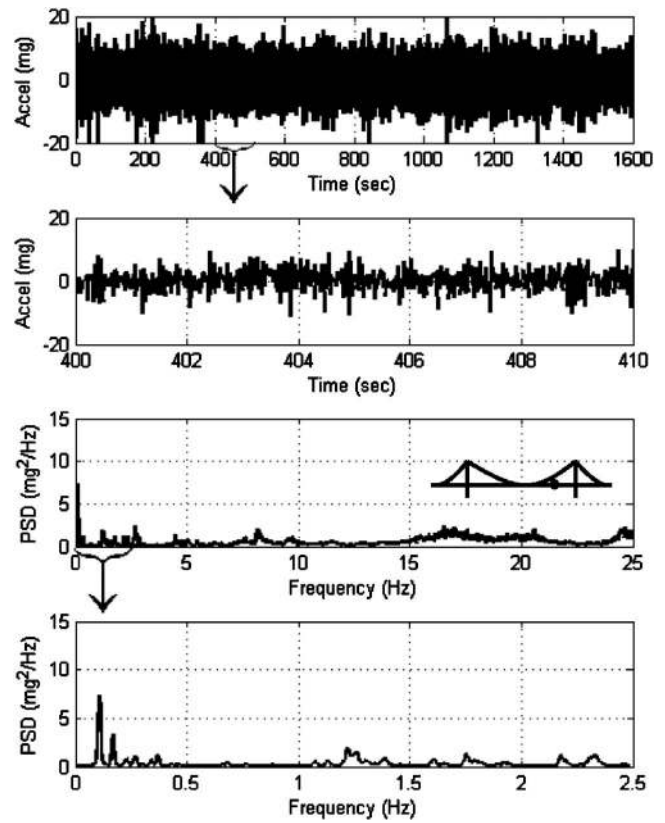
effective bandwidth, loss rate, and average network bandwidth. These three metrics are important indications of network quality and are critical to scalability of the network. The *effective bandwidth* is defined as the amount of data per unit time that is sent to the base station from a node *n*-hops away. Fig. 11 shows the effective bandwidth based on empirical measurements of network performance for four different runs. The one-hop bandwidth of about 1,200 bytes/s is reduced by each additional hop because each node has to receive, buffer, and transmit the packets in the communication stream. A pipeline length of $K=5$ was established for the network, so the effective bandwidth remains relatively constant for nodes that are beyond the fifth node up to the 45th hop, which was the deepest hop of the network. These results show that the data pipelining is very effective for producing a constant effective bandwidth in a large multihop network.

Considering communication packet loss and retransmission, Fig. 12 plots the *loss rate* versus hop count for four runs. Although the loss rate increases as hop count goes up, it is less than 2.5% for 45 hops, which means that the effective volume of transmitted data from the deepest node in the network is only increased slightly due to packet loss. The figure also shows the loss rate for the four runs compared with the estimated loss rates for different values of pipeline length. Using a smaller pipeline length increases the effective bandwidth but the volume of transmitted data increases because interference causes higher losses and more retransmission. In the current deployment $K=5$ provides a good balance between effective bandwidth and loss rate.

Another measure of performance is the *average network bandwidth*, defined as the average amount of data collected during a run per unit time. Fig. 13 shows this metric during the 2-month deployment. In the installation phase only a few nodes were op-

JOURNAL OF INFRASTRUCTURE SYSTEMS © ASCE / MARCH 2008 / **95**

Fig. 9. Time-history and power spectral density for vertical sensor at west-side midspan (run 174, node 78)

Fig. 10. Time-history and power spectral density for vertical sensor at west-side north 1/4–span (run 174, node 45)

erational, and the average network bandwidth was dominated by the effective bandwidth of nodes that are close to the base station. When additional nodes were being installed and the network de-bugged, the average bandwidth fluctuated based on which part of the network was operational and how far the nodes were from the base station. When the entire network was operational, the average bandwidth stabilized at 550 bytes/s, taking full advantage of pipelining. In summary, the empirical data on bandwidth and packet loss in a large-scale deployment show that the pipelining of data is very effective in providing a constant and reliable effective bandwidth for a large number of hops.

Analysis of Vibration Modes

Although the vibration modes of a structure, particularly the lower modes, are not very sensitive indicators of the health of a structure (Doebling et al. 1998), they are useful measures to study the quality of data acquired in the WSN. The ambient vibration data from the Golden Gate Bridge is used to estimate modal properties using off-line modal realization methods. The analysis examines the repeatability of the data and the effect of a spatially dense sensor network on estimated modal properties.

### Modal Identification Methods

The continuous-time dynamic system can be modeled by a multiinput-multioutput (MIMO) system. The system reacts to the input signals $x_1, \ldots, x_p$, and produces response signals $y_1, \ldots, y_q$. A multi-degree-of-freedom mass-damper-spring system is an example of such a system and can be mathematically modeled by

$$M\ddot{U}(t) + C\dot{U}(t) + KU(t) = F(t)$$

where M=mass matrix; C=damping matrix; K=stiffness matrix; $U(t)$=displacement vector; and $F(t)$=external forces.

The objective of the system identification process is to estimate properties of the system transfer function $H(s)$, using the observed input and output response.

A system identification method using multivariate autoregressive models (ARX) is used in this study to estimate modal properties of the bridge (Ljung 1999). The multivariate ARX(M,N) consists of M autoregressive matrices and N exogenous matrices
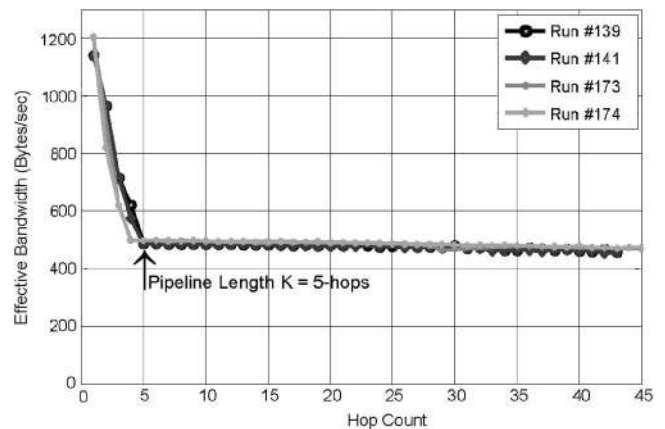
Fig. 11. Effective bandwidth of wireless sensor network with pipelining for four runs
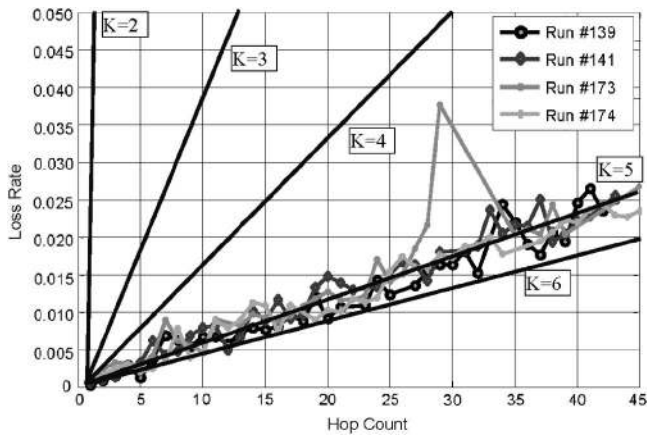
Fig. 12. Network loss rate versus hop count using pipelining for four runs compared with theoretical rates with *K*-nodes pipelining

$$A(q)\bar{y}(n) = B(q)\bar{x}(n) + \bar{e}(n)$$

where $A(q)$ and $B(q)$ = autoregressive- and exogenous operators in discrete time domain, respectively; and $H(q) = B(q)/A(q)$ = discrete system transfer function. The discrete functions $\bar{y}(n)$, $\bar{x}(n)$, and $\bar{e}(n)$ = output, input, and noise vectors, respectively, where $\bar{y}(n) = \bar{y}(nT_0)$, $\bar{x}(n) = \bar{x}(nT_0)$, and T_0 = sampling period. This equation can be rewritten in time domain as

$$\sum_{i=0}^{M} A_i \bar{y}(n-i) = \sum_{i=1}^{N} B_i \bar{x}(n-i) + \bar{e}(n)$$

The discrete-time input and output vectors are p- and q-dimensional vectors $\bar{x}(n) = [x_1(n)\ x_2(n) \cdots x_p(n)]^T$ and $\bar{y}(n) = [y_1(n)\ y_2(n) \cdots y_q(n)]^T$. A_i are $q \times q$ matrices of AR coefficients while B_i are $q \times p$ coefficient matrices of exogenous terms. The noise vector $\bar{e}(n)$ is assumed to be independent and identically distributed (IID). For a MIMO system with measured input and output signals, i.e., known as $\bar{x}(n)$ and $\bar{y}(n)$ for $n = 1, 2, \ldots, k$, a number of computational algorithms to estimate A_i and B_i parameters are described in Ljung (1999). Stochastic (output-only) systems are special cases of this general model, and when the input can be reasonably assumed to have characteristics of white noise, an equivalent autoregressive (AR) or autoregressive with moving average (ARMA) model can be used (Peeters and Roeck 2001). The computational steps for determining the parameters in both
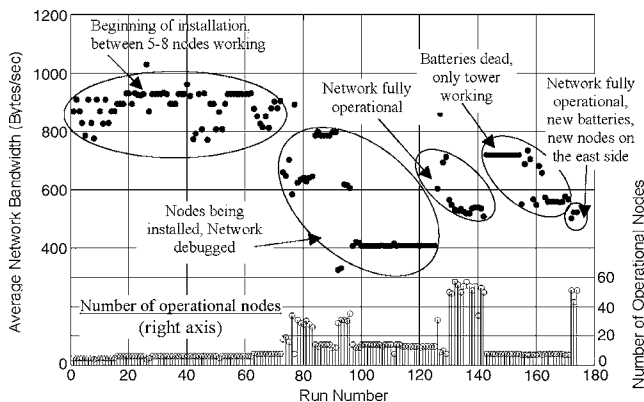
Fig. 13. Average network bandwidth for individual runs of wireless sensor network
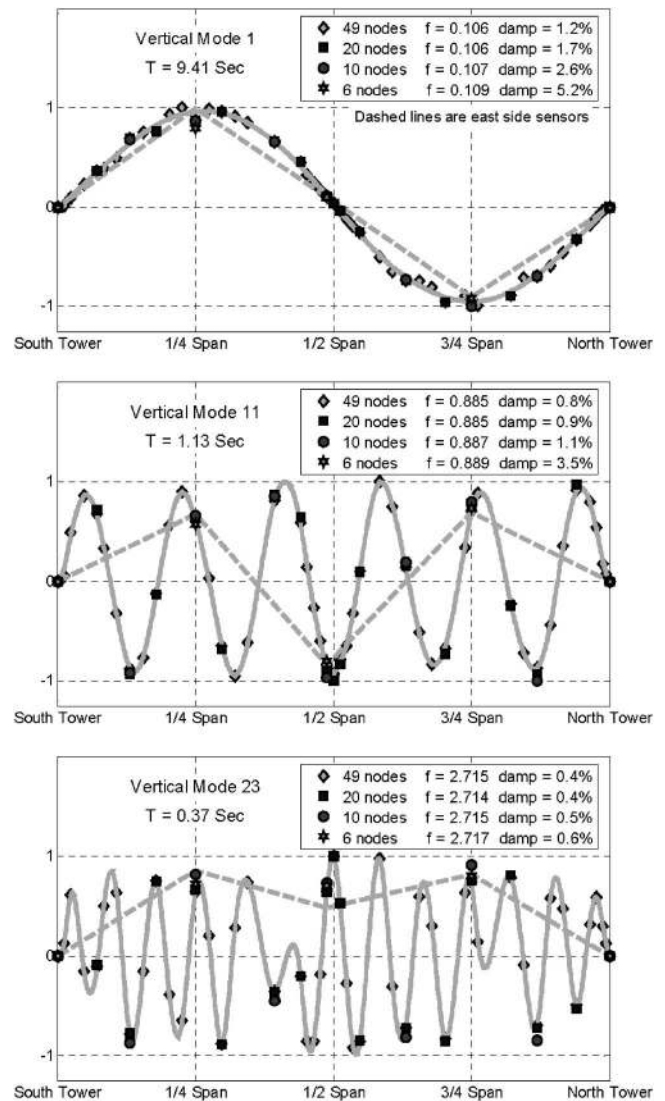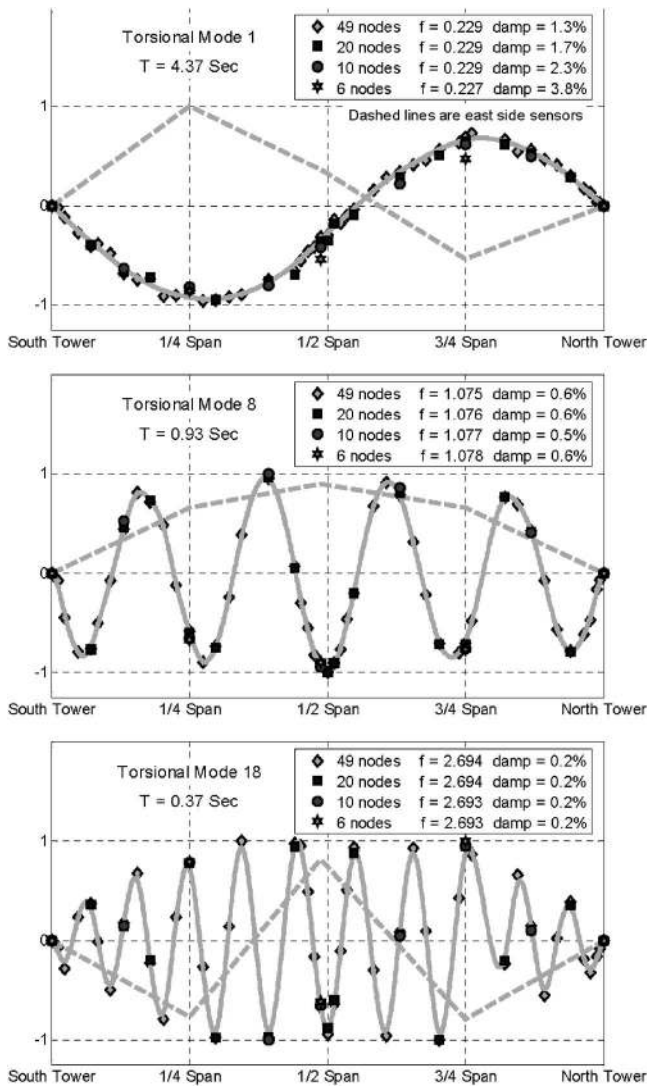

Fig. 14. Estimated vertical mode shapes of main span for four data sets

cases are similar to that of ARX methods (Juang and Phan 2001).

After the modal vibration properties are identified, modal phase collinearity (MPC) is used to distinguish actual modes from spurious ones that are an artifact of the computation. Vibrations of different parts of a structure in a classical normal mode are monophase, i.e., the difference between their phases is either 0 or π. MPC is a measure to quantify this monophase behavior (Pappa et al. 1993). The MPC value for a mode is close to unity for a noise-free set of data. In this study, a cutoff MPC of 0.90 is chosen; however, most of the selected modes have MPC values of above 0.95.

Modal Results for Main-Span

With a 50 Hz sampling rate, the signals have a Nyquist frequency of 25 Hz, but analyzing a large system in this frequency range requires a very high-order model. To reduce model order and concentrate on important vibration modes of the main-span below 5 Hz, the signals were low-pass filtered off-line with a Chebychev Type-II filter with a 5 Hz cutoff frequency and then downsampled accordingly. Figs. 14–17 show several estimated vertical and tor-
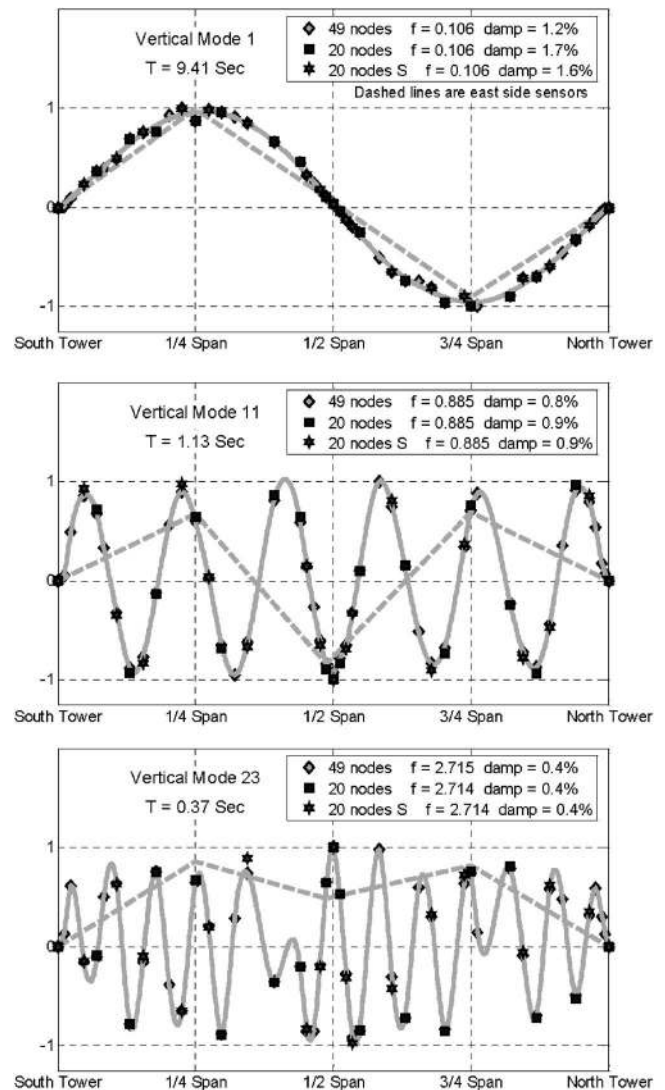
Fig. 15. Estimated torsional mode shapes of main span for four data sets

Fig. 16. Estimated vertical mode shapes of main span for shifted data sets

sional modes with frequencies in the 0–5 Hz frequency band. The various vibration mode estimates shown in the figures are used to evaluate the repeatability of the information in the ambient vibration data.

With a high spatial resolution network on the main-span of the bridge, it is possible to examine how the spatial sampling affects the repeatability of identified vibration properties. Two aspects of node configuration are examined studying relation to the repeatability of modal information: spatial density of the network and shift in node locations. To study *spatial repeatability*, the modal properties using different data sets with different spatial densities are compared. For *shift repeatability*, the modal properties from two different data sets with the same number of nodes but at different locations are compared with reference modal properties estimated using the full network data.

Three modes in vertical and torsional directions are used to examine the effect of spatial resolution in estimated vibration properties: Modes 1, 11, and 23 in the vertical direction, and torsional modes 1, 8, and 18. These modes represent the lower, middle, and higher range of identified frequencies in each direction. Figs. 14 and 15 show the mode shapes, frequencies, and damping ratios of four sets of data. Each set of data consists of a

series of nodes: six nodes in the smallest set, ten nodes in the second set, 20 nodes in the third set, and 49 nodes in the largest set. Each set includes three nodes on the east side of the main-span, and the remaining nodes are on the west side. The east-side nodes are included to distinguish between vertical and torsional modes. The data sets used in spatial repeatability analysis are increasing in size with the doubling of nodes for each subsequent set. The solid lines in the figures are fitted splines to the 49-node data set, which are considered the reference mode shapes. Figs. 14 and 15 show that the mode shapes from all data sets are consistent with the reference shapes. Furthermore, the estimated frequencies are comparable. On the other hand, the estimated damping ratios decrease as the number of nodes used in the system identification increase. This is because the damping estimate is sensitive to measurement noise. As the number of data points increases, the model certainty improves, the effect of noise decreases, and hence the damping ratio estimate decreases.

Repeatability with respect to the location of the nodes gives a different measure of consistency of the collected data, because mutually exclusive data sets with similar sizes can be selected to compare their vibration contents. Using data sets with similar sizes makes the effect of measurement noise in estimated param-
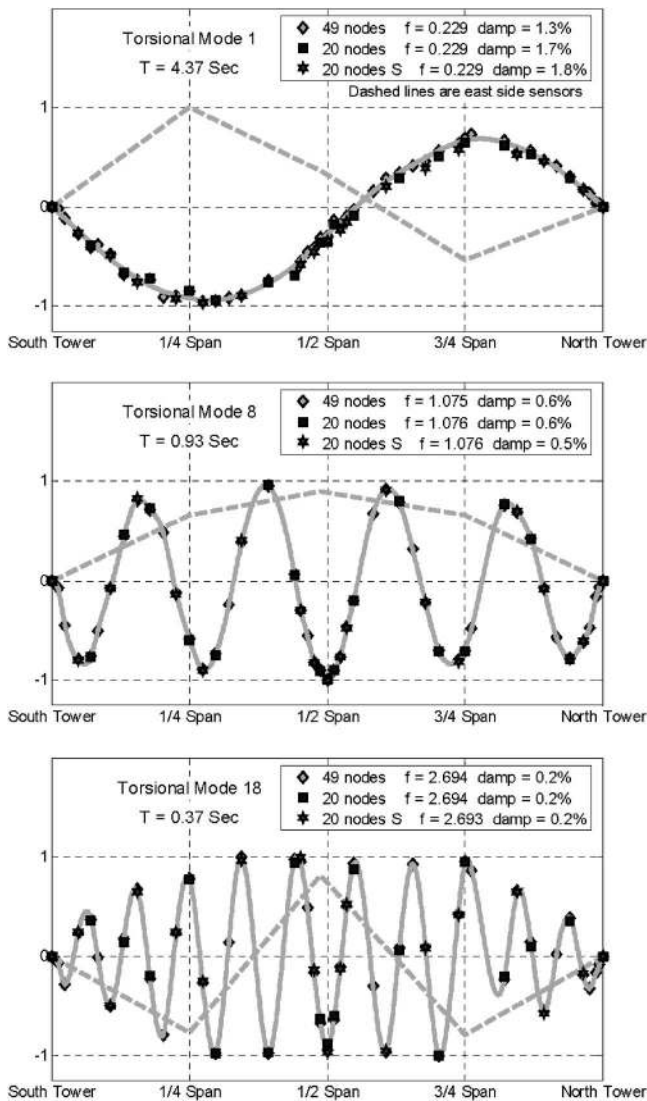
98 / JOURNAL OF INFRASTRUCTURE SYSTEMS © ASCE / MARCH 2008

Fig. 17. Estimated torsional mode shapes of main span for shifted data sets

tion as well as ambient structural vibration. Software components were developed for the TinyOS operating system for reliable command dissemination and data collection and spatial reuse of network bandwidth is implemented through pipelining. Time synchronization for high-frequency sampling is provided by modifying TinyOS components to limit total network jitter.

The performance of the network is analyzed during the testbed deployment on a long-span bridge. The data on network performance confirm the effectiveness of spatial reuse of radio bandwidth through pipelining in maintaining a scalable network. The quality of ambient structural vibration data is investigated by studying the repeatability of the estimated modal properties of the structure with variable numbers and locations of the nodes. The estimated structural modal properties are consistent as the number of nodes increases. The scalable WSN enables a high spatial density network, which makes it possible to identify higher modes of vibration with greater accuracy. The identified modes are also consistent for data sets with different configuration of nodes that independently reflect the vibration properties of the bridge.

Tests and analysis of the hardware and software provided valuable insight in designing real-time WSN for SHM and a roadmap to future work. In order to guarantee a real-time system that can instantly react to commands and triggers, two main principles should be observed in the architecture of software and hardware. First, the operating system needs to be capable of supporting multiple threads to avoid delays of computation and communication tasks while sampling data from the sensors. Second, the hardware needs to be equipped with a separate microcontroller that is dedicated to sampling job, to let a sampling-only process be enforced. This is clearly an extra component in the hardware architecture, which results in more power usage by the node, but is a necessary feature for a real-time WSN. The addition of a second microcontroller also provides more computational power to the node, which can be used for in-network processing to reduce the volume of transmitted data and transform the WSN from a sensing/ routing entity to a parallel computing unit as well.

eters equal. Additionally, using mutually exclusive data sets guarantees that the compatibility of the estimated modal properties by each set is because they independently reflect the vibration properties of the bridge. Two sets of 20 nodes are selected, where the two sets only share one node at the midspan and all other nodes are between 15.25 and 30.5 m apart from each other such that one set is a shifted version of the other set. The same three modes in vertical and torsional directions are considered in Figs. 16 and 17. The plots show shift repeatability in the data, and the estimated frequencies and damping ratios of the two sets match each other and the mode shapes are consistent with the reference mode shape estimated using the full record.

Conclusions

The design, implementation, and deployment of a wireless sensor network for structural health monitoring applications has provided new information about the scalability and performance of the network. Hardware components were developed to provide the range and sensitivity for sensing acceleration from strong mo-

Acknowledgments

References

Abdel-Ghaffar, A. M., and Scanlan, R. H. (1985a). "Ambient vibration studies of Golden Gate Bridge: I. Suspended structure." *J. Eng. Mech.*, 111(4), 463–482.

Abdel-Ghaffar, A. M., and Scanlan, R. H. (1985b). "Ambient vibration studies of Golden Gate Bridge: II. Pier-tower structure." *J. Eng. Mech.*, 111(4), 483–499.

Analog Devices. (1999). "ADXL202 low cost ±2*g* dual axis iMEMS® accelerometer with duty cycle output." ⟨http://www.analog.com/UploadedFiles/Data_Sheets/ADXL202E.pdf⟩.

Buonadonna, P. (2003). "Index of/tinyos-1.x/tos/lib/Broadcast." ⟨http://www.tinyos.net/tinyos-1.x/tos/lib/Broadcast⟩.

Chipcon Products. (2007). "2.4 GHz IEEE 802.15.4/ZigBee-Ready RF Tranceiver (Rev. B)." ⟨http://focus.ti.com/lit/dx/symlink/cc2420.pdf⟩.

Crossbow. (2007a). "MICAz, wireless measurement system."

Crossbow. (2007b). "iMote2, high-performance wireless sensor network node." ⟨http://www.xbow.com/Products/Product_pdf_files/Wireless_pdf/Imote2_Datasheet.pdf⟩.

Doebling, S. W., Farrar, C. R., and Prime, M. B. (1998). "A summary review of vibration-based damage identification methods." *Shock Vib. Dig.*, 30(2), 91–105.

Doebling, S. W., Farrar, C. R., Prime, M. B., and Shevitz, D. W. (1996). "Damage identification and health monitoring of structural and mechanical systems from changes in their vibration characteristics: A literature review." *Rep. No. LA-13070-MS*, Los Alamos National Laboratory, Los Alamos, N.M.

Farrar, C. R. (2001). "Historical overview of structural health monitoring." *Lecture notes on structural health monitoring using statistical pattern recognition*, Los Alamos Dynamics, Los Alamos, N.M.

Hill, J., Gay, D., and Levis, P. (2003). "index of tinyos-1.x/tos/system." ⟨http://www.tinyos.net/tinyos-1.x/tos/system⟩.

Hill, J., Szewczyk, R., Woo, A., Hollar, S., Culler, D. E., and Pister, K. S. J. (2000). "System architecture directions for networked sensors." *Proc., 9th Int. Conf. on Architectural Support for Programming Languages and Operating Systems (ASPLOS 2000)*, Cambridge, Mass., 93–104.

Ihler, E., Zaglauer, W., Herold-Schmidt, U., Dittrich, K. W., and Wiesbeck, W. (2000). "Integrated wireless piezoelectric sensors." *Proc. SPIE*, 3(991), 44–51.

Juang, J. N., and Phan, M. Q. (2001). *Identification and control of mechanical systems*, Cambridge University Press, Cambridge, U.K.

Kim, S., Fonseca, R., Kumar Dutta, P., Tavakoli, A., Culler, D. E., Levis, P., Shenker, S., and Stoica, I. (2006). "Flush: A reliable bulk transport protocol for multihop wireless network." *Technical Rep. No. UCB/EECS-2006-169*, University of California, Berkeley, Calif.

Kim, S., Pakzad, S. N., Culler, D., Demmel, J., Fenves, G. L., Glaser, S., and Turon, M. (2007). "Health monitoring of civil infrastructures using wireless sensor networks." *Proc., 6th Int. Conf. on Information Processing in Sensor Networks (IPSN 2007)*, Cambridge, Mass.

Ljung, L. (1999). *System identification—Theory for the user*, 2nd Ed., Prentice-Hall, Upper Saddle River, N.J.

Lynch, J. P., and Loh, K. J. (2006). "A summary review of wireless sensors and sensor networks for structural health monitoring." *Shock Vib. Dig.*, 38(2), 91–128.

Lynch, J. P., Sundararajan, A., Law, K. H., Kiremidjian, A. S., Carryer, E., Sohn, H., and Farrar, C. R. (2003). "Field validation of a wireless structural health monitoring system on the Alamosa Canyon Bridge." *Proc. SPIE*, 5057, 267–278.

Lynch, J. P., Wang, Y., Law, K. H., Yi, J.-H., Lee, C. G., and Yun, C. B. (2005). "Validation of a large-scale wireless structural monitoring system on the Geumdang Bridge." *Proc., Int. Conf. on Safety and Structural Reliability (ICOSSAR)*, Rome, Italy.

Mainwaring, A., Polastre, J., Szewczyk, R., Culler, D., and Anderson, J. (2002). "Wireless sensor networks for habitat monitoring." *Proc., 2002 ACM Int. Workshop on Wireless Sensor Networks and Applications, WSNA'02*, Atlanta.

Maróti, M., Kusy, B., Simon, G., and Lédeczi, Á. (2004). "The flooding time synchronization protocol." *Proc. ACM 2nd Int. Conf. on Embedded Networked Sensor Systems (SenSys 2004)*, Baltimore, 39–49.

Maser, K., Egri, R., Lichtenstein, A., and Chase, S. (1996). "Field evaluation of a wireless global bridge evaluation and monitoring system." *Proc., 11th Conf. on Engineering Mechanics*, Vol. 2, Fort Lauderdale, Fla., 955–958.

Mastroleon, L., Kiremidjiana, A. S., Carryerb, E., and Law, K. H. (2004). "Design of a new power-efficient wireless sensor system for structural health monitoring." *Proc. SPIE*, 5395, 51–60.

Oppenheim, A. V., and Schafer, R. W. (1999). *Discrete-time signal processing*, 2nd Ed., Prentice-Hall, Upper Saddle River, N.J.

Paek, J., Chintalapudi, K., Cafferey, J., Govindan, R., and Masri, S. (2005). "A wireless sensor network for structural health monitoring: Performance and experience." *Proc., 2nd IEEE Workshop on Embedded Network Sensors (EmNetS-II)*, Sydney, Australia.

Pakzad, S. N., and Fenves, G. L. (2004). "Structural health monitoring applications using MEMS sensor networks." *Proc., 4th Int. Workshop on Structural Control*, Columbia Univ., New York, 47–56.

Pakzad, S. N., Kim, S., Fenves, G. L., Glaser, S. D., Culler, D. E., and Demmel, J. W. (2005). "Multipurpose wireless accelerometers for civil infrastructure monitoring." *Proc., 5th Int. Workshop on Structural Health Monitoring (IWSHM 2005)*, Stanford, Calif.

Pappa, R. S., Elliott, K. B., and Schenck, A. (1993). "Consistent mode indicator for eigen system realization algorithm." *J. Guid. Control Dyn.*, 16(5), 852–858.

Peeters, B., and Roeck, G. D. (2001). "Stochastic system identification for operational modal analysis: A review." *J. Dyn. Syst., Meas., Control*, 123, 659–667.

Pei, J.-S., Kapoor, C., Graves-Abe, T. L., Sugeng, Y., and Lynch, J. P. (2005). "Critical design parameters and operating conditions of wireless sensor units for structural health monitoring." *Proc., 23rd Int. Modal Analysis Conf. (IMAC XXIII)*, Orlando, Fla.

Ruiz-Sandoval, M., Nagayama, T., and Spencer, B. F. (2006). "Sensor development using Berkeley Mote platform." *J. Earthquake Eng.*, 10(2), 289–309.

Silicon Design (2007). "Model 1221, low noise analog accelerometer." ⟨http://www.silicondesign.com/pdf⟩.

Smyth, A. W., Pei, J., and Masri, S. F. (2003). "System identification of the Vincent Thomas suspension bridge using earthquake records." *Earthquake Eng. Struct. Dyn.*, 32, 339–367.

Sohn, H., and Farrar, C. R. (2000). "Statistical process control and projection techniques for damage detection." *Proc., European COST F3 Conf. on System Identification and Structural Health Monitoring*, Madrid, Spain, 105–114.

Strubbs, N., Sikorsky, C., Park, S. C., and Bolton, R. (1999). *Verification of a methodology to nondestructively evaluate the structural properties of bridges*, Structural Health Monitoring Workshop, Stanford Univ., Palo Alto, Calif., 440–449.

TinyOS. (2007). "TinyOS community forum, and open-source for the networked sensor regime." ⟨http://www.tinyos.net/⟩.

Tolle, G., et al. (2005). "A macroscope in the redwoods." *Proc., 3rd ACM Conf. on Embedded Networked Sensor Systems (Sensys 05)*, San Diego.

Wang, G., and Pran, K. (2000). "Ship hull structure monitoring using fiber optic sensors." *Proc., European COST F3 Conf. on System Identification and Structural Health Monitoring*, Madrid, Spain, 15–27.

Welch, P. D. (1967). "The use of fast Fourier transform for the estimation of power spectra: A method based on time averaging over short, modified periodograms." *IEEE Trans. Audio Electroacoust.*, 15(2), 70–73.

Westermo, B., and Thompson, L. D. (1997). "A peak strain sensor for damage assessment and health monitoring." *Structural health monitoring, Current status and perspectives*, Stanford University Press, Palo Alto, Calif., 515–526.

Williams, E. J., and Messina, A. (1999). "Applications of the multiple

damage location assurance criterion." *Proc., Int. Conf. on Damage Assessment of Structures*, Dublin, Ireland, 256–264.

Woo, A., Tong, T., and Culler, D. (2003). "Taming the underlying challenges of reliable multihop routing in sensor networks." *Proc., SenSys 2003*, Los Angeles.

Ying, L., Kiremidjian, A. S., Nair, K. K., Lynch, J. P., and Law, K. H. (2005). "Algorithms for time synchronization of wireless structural monitoring sensors." *Earthquake Eng. Struct. Dyn.*, 34, 555–573.

Zimmermann, D. C. (1999). "Looking into the crystal ball: The continued need for multiple viewpoints in damage detection." *Damage Assessment of Structures, Proc., Int. Conf. on Damage Assessment of Structures*, Dublin, Ireland, 76–90.